Development and Characterisation of Completely Degradable Composite Tissue Engineering Scaffolds

PhD Thesis by Montse Charles-Harris Ferrer

PhD Supervisor: Josep A. Planell i Estany

Barcelona, July 2007

Chapter 4: Study of the degradation of composite scaffolds made via Solvent Casting and Phase Separation

Introduction

Biodegradability is a critical aspect of the composite foams developed in this thesis. Biodegradability offers the advantage of reducing many problems associated to tissue replacement such as rejection and chronic inflammation. Both the PLA and the calcium phosphate glass are completely degradable in physiological conditions[1]. Although conclusions derived from *in vitro* assays are not extrapolable to *in vivo* conditions, they do offer valuable information on the potential *in vivo* behaviour of the material. An *in vitro* degradation study is thus an essential step in the characterisation of a tissue engineering device.

The degradation rate of a tissue engineering scaffold should ideally be similar or slower than the rate of tissue repair. Furthermore, its degradation by-products should not be harmful or toxic to the body and must be excreted easily through normal physiological pathways[2]. Various studies have characterised the evolution of scaffold properties during degradation in *in vitro* conditions. These studies typically use a buffer solution such as simulated body fluid (SBF), or phosphate buffered saline (PBS) to maintain a stable pH, and perform the assay at 37ºC. The scaffolds remain in solution for a certain number of days or weeks, and various parameters such as; weight loss, polymer molecular weight and mechanical properties are monitored[3-6].

Many factors are found to influence the degradation profile of polymeric scaffolds (Table 4.1), ranging from the properties of the polymer to the design of the implant. The presence of a filler also affects degradation either by creating physical barriers between the polymer and the buffer or by altering the pH of the medium with its own degradation by-products.

Factors that influence polymeric scaffold degradation *in vitro*
Polymer molecular weight
Polymer polydispersity
Polymer crystallinity
Size of the device
Morphology and porosity of the device (thickness of pore walls)
pH of the degradation medium
Buffering capacity of the degradation medium
Degradation conditions (static or dynamic)
Thermal history or processing of the device

Table 4.1: List of factors that can affect the degradation of polymeric scaffolds *in vitro*. Adapted from [2;7-9]

The degradation process of the scaffolds can be modulated or controlled by optimising scaffold material, design and dimensions. Although i*n vitro* conditions are meant to imitate the milieu the scaffolds will be implanted in *in vivo*, there are many differences between the two. Indeed, scaffolds implanted *in vivo* will be exposed to many other elements, which often accelerate degradation[10] (Table 4.2). Thus, *in vitro* studies should be considered a first step in scaffold degradative characterisation, to be completed with cytotoxicity tests, *in vitro* cell cultures and finally *in vivo* implantation.

Factors that affect degradation *in vivo*
Presence of enzymes
Cellular activity
Cell-induced pH changes
Presence of proteins

Table 4.2: List of factors that affect scaffold degradation in vivo. Adapted from [10].

PLA can be degraded *in vivo* either by hydrolysis in contact with an aqueous medium, or by phagocytosis by macrophages. Hydrolysis is the dominant degradative mode. Once PLA is placed in contact with an aqueous medium, it absorbs H_2O. The

H_2O diffuses rapidly throughout the structure and begins the hydrolysis of the ester bonds homogeneously. The cleavage of an ester bond yields a carboxyl and a hydroxyl end group. Thus, degradation causes an increase in the number of carboxylic chain ends which decrease the pH and catalyse hydrolysis. The polymer backbone is thus cleaved into water soluble oligomers and lactic acid monomers. The oligomers and monomers which are close to the surface in contact with the buffer, can dissolve into the medium easily. Those found towards the center of the matrix, however, remain trapped within the structure and contribute to the autocatalytic effect[9;11;12]. Thus the molecular weight of the PLA decreases during the first weeks of degradation, though the overall weight of the sample may not vary significantly[12].

This autocatalytic effect, explains the size-dependent degradation profile that PLA devices show. In effect, thin devices or fibres, will degrade slower than bulky structures because the autocatalytic effect will not occur in the former. Indeed, highly porous scaffolds degrade slower than non-porous scaffolds[4]. Thus, the complete degradation of a PLA implant may take from months to years depending on its design and thickness. Bulky solid structures often show no evidence of degradation on their surface and are in fact hollow after several weeks of degradation. Table 4.3 shows a list of factors that specifically influence the degradation profile of PLA *in vitro*.

pH of the medium	Both acids and bases can accelerate PLA hydrolysis
Porosity	High porosities reduce the autocatalytic effect because the oligomers can attain the surrounding medium easily
Molecular weight	High molecular weights imply slower degradation
Crystallinity	Crystalline regions are more resistant to degradation than the amorphous regions
Glass transition temperature (Tg)	The lower the glass transition temperature, the higher the mobility of the polymer chains. Thus H_2O can penetrate the structure easier and hydrolysis can occur earlier

Table 4.3: Factors that affect PLA degradation [7;9]

The second phase of the composite material, i.e. the calcium phosphate glass is also resorbable. One of the advantages of calcium phosphate glasses as opposed to

calcium phosphate crystalline solids, is the possibility of tailoring their solubility by means of their chemical composition. The G5 glass used in this study contains titanium, sodium and calcium ions as network modifiers. Titanium, having a small radius and a high ionic charge, decreases the solubility and increases the mechanical properties of the glass[13].

The G5 glass' degradation profile depends on the surface/volume ratio the assay is performed in: the ratio between the surface of the glass exposed to the medium, and the volume of liquid it is submerged in. At a 1ml/ cm^2 ratio, the G5 glass loses less than 0.2% of its initial weight after 100 days in SBF and its elastic modulus barely varies during this time. Its dissolution pattern is divided into two stages; a slow dissolution for the first 100 days, followed by a faster dissolution from then onwards. It was found to degrade ten times slower in SBF than in distilled water due to the buffering effect of the SBF[14].

The aim of the degradation study was to characterise the physico-chemical degradation of the PLA- G5 glass scaffolds and thus better understand their behaviour during *in vitro* cell cultures and eventually *in vivo*. The scaffolds were submerged in SBF during ten weeks at 37°C. Every two weeks, samples were removed from the SBF and characterised. General macroscopic properties such as morphology, porosity, mechanical properties and total weight loss were measured. The degradation of the glass particles in the scaffolds was surveyed by measuring the total glass particle content and the dissolution of glass in the SBF. The behaviour of the PLA was monitored by performing Differential Scanning Calorimetry (DSC) and analysing different parameters such as the PLA's glass transition temperature, its crystallinity and its melting point.

Materials and Methods

Materials

The scaffolds used for the degradation study were those developed in chapters 2 and 3, their compositions can be seen in Table 4.4. The PLA and G5 glass they are composed of have been described in detail in Chapter 2. They both contained 5

weight/volume percent (w/v%) of PLA in the solvent and 50 weight percent (wt%) of glass particles sieved below 40μm.

.	**Solvent Casting**	**Phase Separation (quenched at –20°C)**
PLA w/v%	5%	5%
Solvent used	Chloroform	Dioxane (95%) + H_2O (5%)
Glass wt%	50%	50%
Glass particle size (μm)	<40	<40
NaCl particle size (μm)	[80-120]	/
Porosity	~95%	~89%
Pore size (μm)	*	~140

Table 4.4: Composition of the scaffolds used in the degradation study. * The exact pore size of the solvent cast scaffolds cannot be calculated due to the extreme high porosity, in any case, the NaCl particle size (80-120 μm) can be considered the lower bound.

In order to imitate the *in vitro* environment, the scaffolds were immersed in pH=7.25 SBF at 37°C for ten weeks. SBF is an acellular solution whose ionic composition is very similar to that of human blood plasma (Table 4.5). It was developed by Kokubo[15] in order to simulate the *in vivo* milieu bioceramic implants would be surrounded by. Although SBF's initial aim was to imitate blood plasma, it lacks many elements such as proteins, CO_2, and other organic molecules which play an important role in material behaviour *in vivo*. SBF is now mainly used to evaluate the bioactivity of biomaterials[16;17], i.e. whether they develop a carbonated hydroxyapatite layer on their surface which forms a uniting interface with the surrounding tissue (see Introduction, Chapter 1). In the case of this study, SBF was used to provide a reproducible *in vitro* milieu in which to study the degradation of the materials. The occurrence of precipitates was evaluated by Scanning Electron Microscopy (SEM) but it was not the main goal of the study.

The SBF was prepared in the laboratory following an internal protocol and filtered with a 0.22μm sterilising filter before storage. Special attention was paid to the cleanliness of the labware used to prepare and store the solutions in order to avoid

contaminations during the 10-week degradation period. Scaffold dimensions were chosen according to the requirements of each test. Scaffolds were submerged in SBF in polyethelyene bottles under a laminar flow hood, and stored in an oven at 37°C. Polyethylene nets were used to prevent the scaffolds from floating during the first weeks of the experiment. The weight/volume ratio between the scaffolds and the SBF was 1/250. The SBF was changed weekly under a laminar flow hood. The samples used for the various tests were taken out of the SBF every two weeks, and dried at 37°C in the oven for two days before testing.

Ion	Concentration (mmol/dm^3)	
	SBF	Human blood plasma
Na^+	142.0	142.0
K^+	5.0	5.0
Mg^{2+}	1.5	1.5
Ca^{2+}	2.5	2.5
Cl^-	147.8	103.0
HCO^{3-}	4.2	27.0
HPO_4^{2-}	1.0	1.0
SO_4^{2-}	0.5	0.5

Table 4.5: Ionic composition of the SBF used in the degradation study and that of human blood plasma.

Methods

Morphology

A qualitative study of the changes in scaffold morphology during the 10-week degradation period was performed by Scanning Electron Microscopy (SEM) on a Jeol JSM-6400.

Mechanical properties

Compression tests were performed on different testing machines for the solvent cast scaffolds or the phase separated ones, due to the differences in stiffness between the two and the availability of adequate load cells.

The solvent cast scaffolds were tested in compression as described in Chapter 2, on an Adamel Lhomargy universal testing machine, with a 100N load cell, at a constant crosshead speed of 2mm/min until 50% strain. All compression samples had a diameter of 12mm. The height of the samples was approximately 10mm.

The phase separated scaffolds were tested on a Bionix 858 servohydraulic testing machine, with a 2.5kN load cell, at a constant crosshead speed of 2mm/min until 50% strain. The stiffness was calculated by the MTS software associated to the testing machine, as the initial linear portion of the stress-strain curve. All compression samples had a diameter of 16mm, the height of the samples varied between 5 and 10 mm.

The difference between the diameters of the solvent cast and phase separation samples was due to their different processing methods and limitations in the availability of processing materials. Solvent cast samples were punched out of a dried paste, whereas phase-separated samples were made in moulds (see Chapters 2 and 3).

Measurements are presented as an average of five samples.

Total Weight Loss

The total weight loss of the scaffolds was measured with three samples that remained in the SBF for the ten weeks. The samples were dried at 37°C for two days (until their mass was stable) and weighed every two weeks on a precision balance in order to calculate the % weight loss (equation {1}). The rate of weight loss between two weeks was also calculated by comparing the percentage of weight remaining (equation {2}).

$$\%wt_{loss} = \frac{w_0 - w_i}{w_0} \qquad \{1\}$$

$$\%wt_{loss}rate = \frac{\dfrac{\%wt^{i}_{loss} - \%wt^{i+2}_{loss}}{\%wt^{i}_{loss}}}{14days} \qquad \{2\}$$

Where; $\%wt_{loss}^{i}$, stands for the percentage weight loss at any given week i, and w_i, stands for the weight at any given week i. The weight loss was divided by 14 days in order to obtain the rate per day.

Glass particle content

The evolution of the glass particle content of the scaffolds during the degradation was measured following the UNE 53-090 protocol to measure the ash content of plastic materials[18]. This method is called calcination and is also used to determine the mineral content of bone. The composite scaffolds are placed in crucibles, weighed ($w_{scaffold}$), and heated with a bunsen burner until the molten polymer releases no more smoke. The crucibles are then placed in an oven and heated for 3 hours at 600°C. After the calcination, the PLA has been entirely transformed into volatile substances, whereas the glass has not suffered siginifcant weight losses. Thus, the material remaining in the crucibles(w_{glass}) is weighed and divided by the initial weight of the scaffolds in order to compute the real glass wt%.

$$Glasswt\% = \frac{w_{Glass}}{w_{Scaffold}} \times 100 \qquad \{3\}$$

The PLA wt% is simply calculated by subracting the glass wt% from 1:

$$\text{PLA wt\%} = 1 - \text{glass wt\%} \qquad \{4\}$$

The results of the total weight loss and the glass particle content can be combined to compute the total glass weight loss ($\%Glasswt_{loss}$) each week (equation nº6), where w_i, stands for the weight of the scaffolds at any given week i, and $\%wt_{loss}^{i}$, stands for the total weight loss as defined in equation {1}. The PLA weight loss can be calculated by substituting the *glasswt%* by that of the PLA in equation nº6.

$$\%Glasswt_{loss}^{i} = \frac{Glasswt\%^{0} - (1 - \%wt_{loss}^{i}) \times Glasswt\%^{i}}{Glasswt\%^{0}} \qquad \{5\}$$

Measurements are presented as an average of three samples.

Porosity

The porosity of the scaffolds was measured by mercury pycnometry every two weeks. The apparent density of the scaffold ($\rho_{scaffold}$) was measured by means of the

volume of mercury it displaced when submerged. The porosity of the scaffold is calculated by dividing its apparent density by the density of the solid composite (ρ_{solid}). In this case, ρ_{solid} was re-calculated every two weeks using the real glass wt% as given by the calcination tests in order to include the variations in glass and polymer wt% with degradation :

$$\%Porosity = 100\left(1 - \frac{\rho_{scaffold}}{\rho_{solid}}\right) \qquad \{6\}$$

Measurements are presented as an average of five samples.

Inductively Coupled Plasma readings

ICP analysis was used to follow the dissolution of the glass particles in the SBF by means of the detection of the titanium ion. The titanium ion was chosen because the other ions present in the G5 glass: calcium, phosphorus and sodium are also found in the SBF.

9.9 ml of SBF from the polyethylene bottles with the scaffolds was withdrawn every two weeks before changing the SBF. The SBF was filtered with a 0.22μm filter, and was stabilised with 100μl of nitric acid to avoid precipitation. The solutions were then measured in triplicate.

Differential Scanning Calorimetry

The thermal transitions of the scaffold material were measured using Differential Scanning Calorimetry (DSC), on a 2029 TA Instruments calorimeter. The samples used weighed between 10 and 15 mg and were submitted to two heating and cooling cycles at 10°C/min:

- First heating ramp: from 10°C to 200°C at 10°C/min. During this ramp, the material displays information on its actual physical and morphological state. This ramp is used to evaluate the heat of fusion, H_f, and melting temperature, T_m, of the material.
- Isothermal for 5 minutes at 200°C to erase all thermal history
- Cooling ramp: from 200°C to 10°C at 10°C/min

- Second heating ramp: from 10°C to 200°C at 10°C/min. This ramp is used to study the polymer equilibrium state properties irrespective of their thermal history. It is used to evaluate the Glass Transition Temperature, T_g, which is indicative of polymer chain length and thus polymer degradation. The crystallisation enthalpy, H_c, and temperature, T_c, are also recorded during the second heating ramp.

The DSC curves were analysed with the Universal Analysis 200 software associated to the calorimeter.

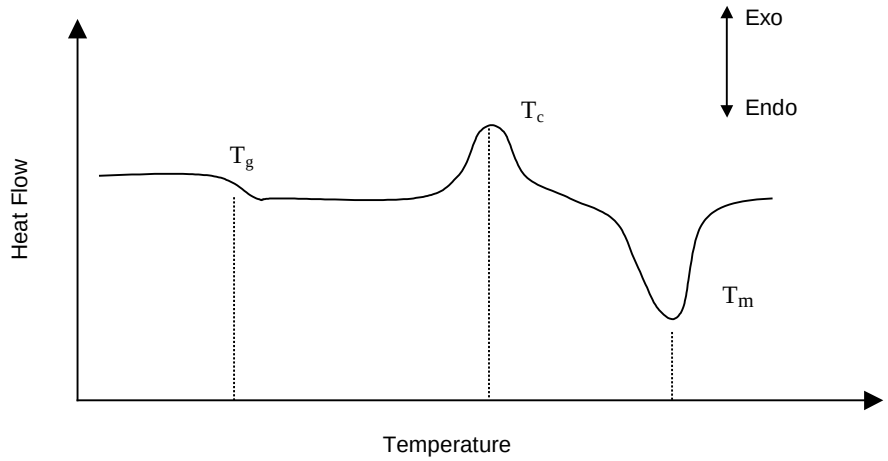

Figure 4.1 shows a schematic diagram of a heat flow curve of the composite scaffolds. The glass transition temperature, T_g, appears as an inflection in the heat flow curve, it is defined as the inflection point of the region. It is measured during the second heating ramp and only concerns the amorphous regions of the polymer.

Crystallisation is an exothermal transition, it occurs at temperatures slightly lower than the melting point of the polymer. The crystallisation of a polymer depends on the capacity of its chains to move and form a crystalline structure. There can be a crystallisation peak in both the first and the second heating ramp. The H_c in the second heating ramp is indicative of polymer chain length. The crystallisation temperature and enthalpy are defined as the maximum of the crystallisation peak and the area under the crystallisation curve respectively.

Melting is an endothermal transition, the melting point is defined as the mininum of the melting peak. The melting point of the PLA used for this study ranges between 163.4-172.4°C as given by the manufacturers (see Chapter 2). The heat of fusion is the

area under the melting peak. Melting is measured during the first heating ramp. Only the crystalline regions of the PLA have a melting temperature.

The heat of fusion is thus used to compute the percentage crystallinity, X_c, of the PLA as the ratio between the H_f of the PLA in the scaffold, and the theoretical H_f value of a 100% crystalline monodispersed L-PLA (H_m^0 = 93.1 J/g), as reported by Fischer[19]. If crystallisation occurs during the first heating ramp, its H_c must be subracted from the H_f value so as to avoid including the PLA that has crystallised during the heating in the total PLA crystallinity:

$$\%X_c = \frac{\Delta H_m - \Delta H_c}{\Delta H_m^0} \times \frac{1}{PLAwt\%} \quad \{7\}$$

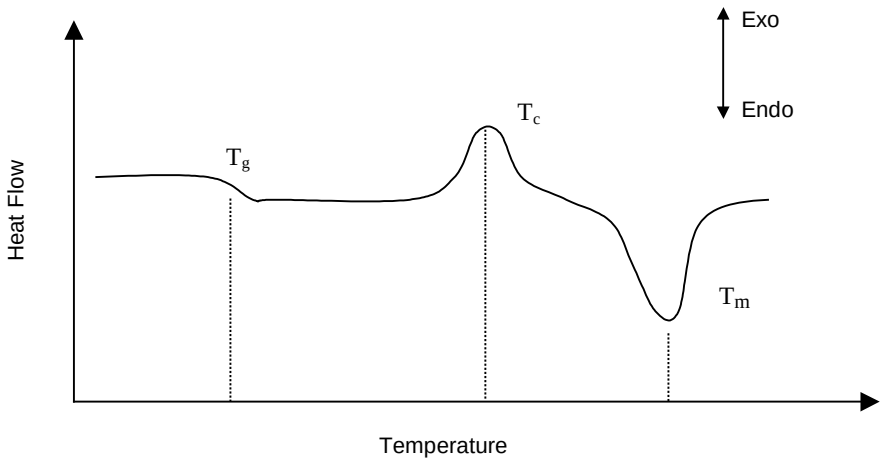

Figure 4.1:
Schematic diagram of a heat flow curve showing the glass transition temperature, T_g, the crystallisation temperature, T_c, and the melting point, T_m.

Measurements were performed in triplicate.

Statistics

The statistical significance of the differences between the averages of the results for all parameters studied was calculated using ANOVA tables with a Fisher multiple comparison test. Statistical significance was established at $p < 0,05$. These calculations have been performed with MINTAB™ Release 14 Minitab Inc. software. Results whose

difference is not statistically significant are indicated with a horizontal line on the graphs.

Results

The ten-week degradation assay was performed for both solvent cast and phase separated scaffolds. Although the scaffolds floated in the SBF in the beginning of the experiment, they all sunk after two to three weeks of degradation. The SBF solution, which is initially colourless, became increasingly yellow and released an odour of cheese or spoilt milk as the degradation proceeded. No contamination by bacteria or fungi was detected during the study. From week eight onwards, some scaffolds had become too fragile to test.

Morphology

In the case of the solvent cast scaffolds, low-magnification (×250) SEM images of the scaffolds did not reveal noticeable differences in morphology during the ten-week degradation period. Close-up views, however, revealed signs of degradation on both the polymer and the glass particles. In effect, Figure 4.2c, shows the glass particle surface which seems to be cracking and detaching from the bulk of the particle. Figure 4.2d shows the PLA pore-wall looking more torn and grooved than before degradation. Qualitatively, the scaffolds lost consistency and tended to crumble when touched towards the end of the degradation.

The phase-separated scaffolds did not show visible signs of degradation (Figure 4.3). The pore walls and glass particles have similar apperances before and after degradation.

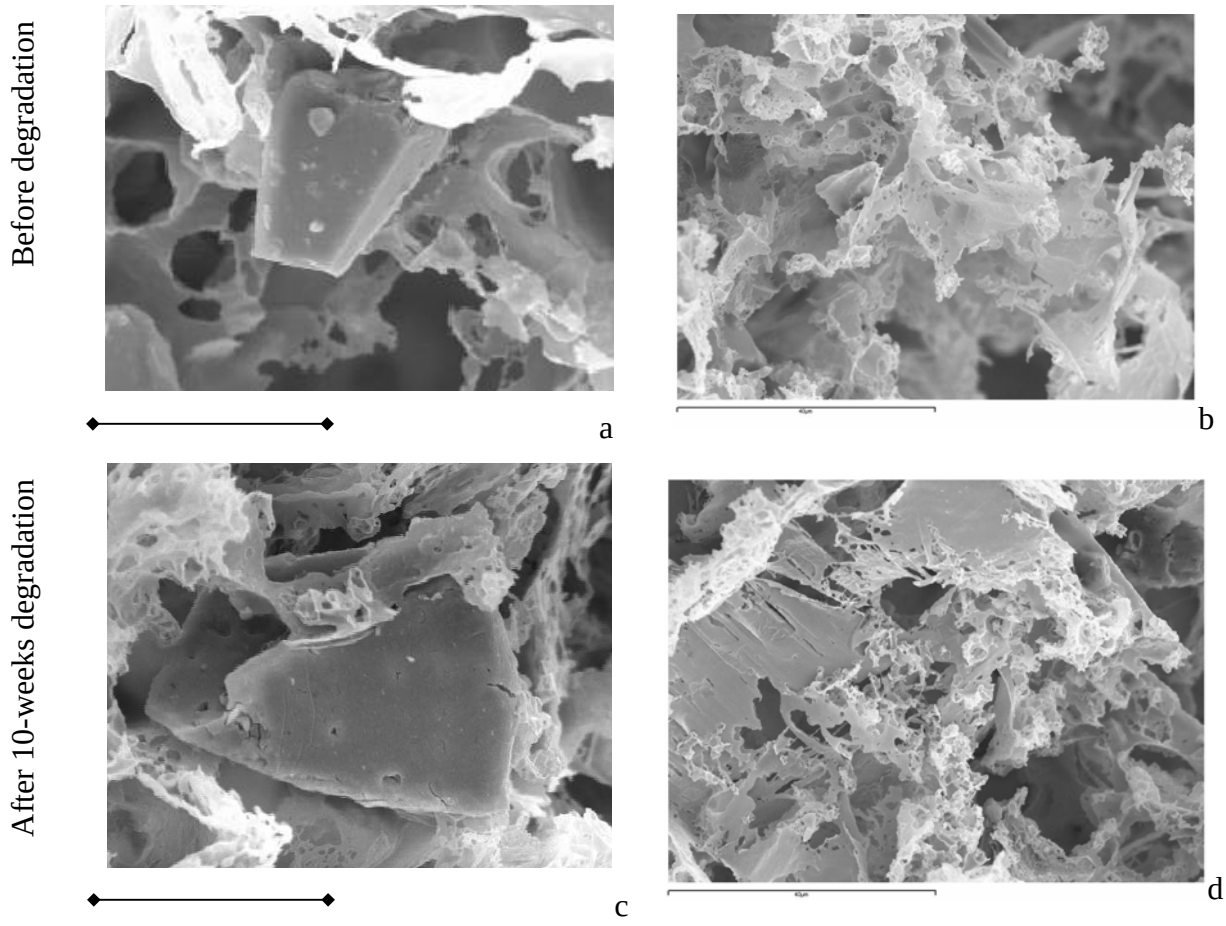

Figure 4.2: SEM images of the solvent cast scaffolds: a) and b), before degradation and c) and d), after ten-weeks of degradation in SBF. Images a) and c) show close-ups of glass particles. Images b) and d) show the PLA pore walls. (Magnification bars for images a) and c) correspond to 20 μm, those for images b) and d) correspond to 40 μm.)

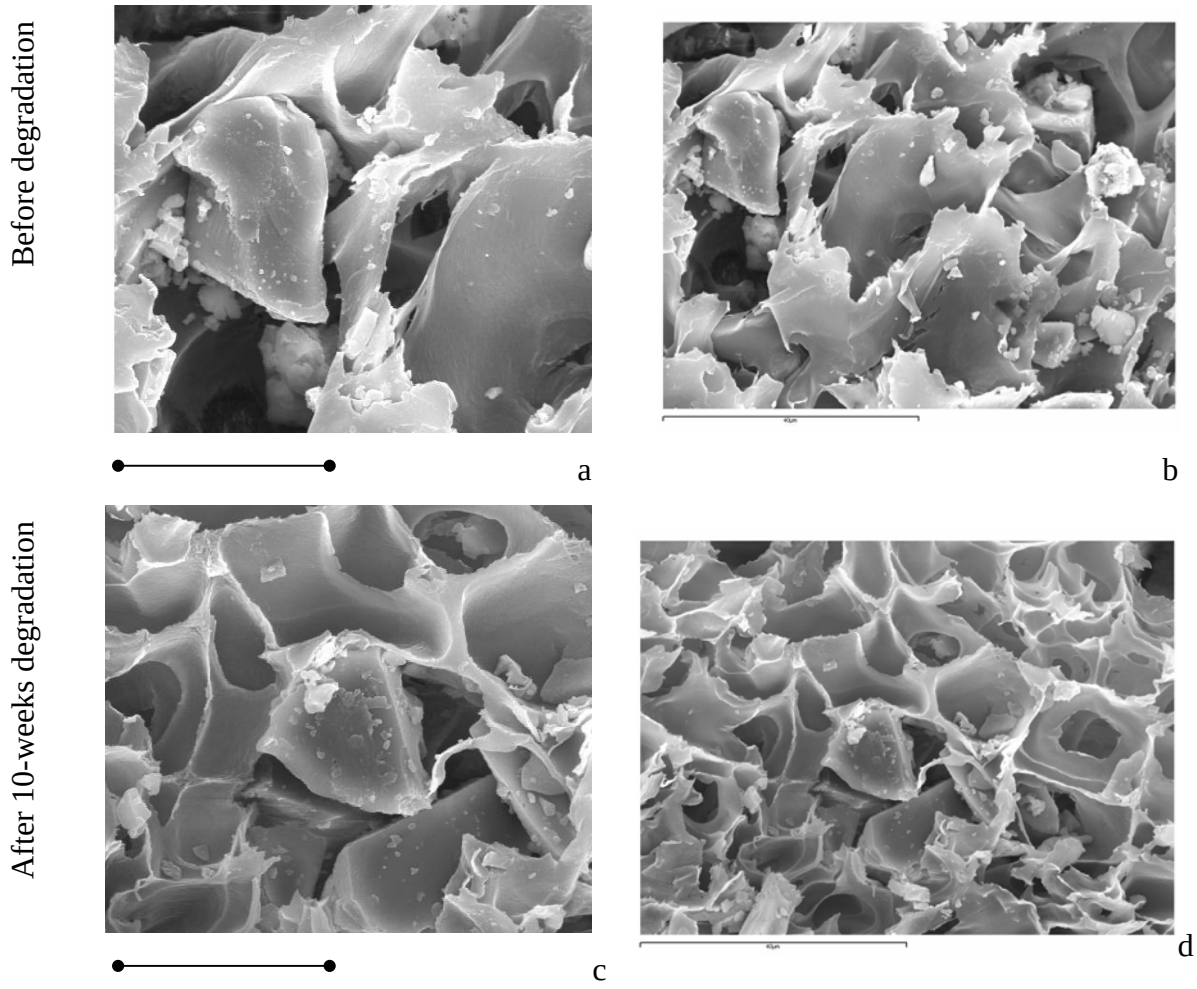

Figure 4.3: SEM images of the phase-separated scaffolds: a) and b), before degradation, and c) and d), after ten-weeks of degradation in SBF. Images a) and c) show close-ups of glass particles. Images b) and d) show the PLA pore walls. (Magnification bars for images a) and c) correspond to 20 μm, those for images b) and d) correspond to 40 μm.)

Porosity

The porosity of the solvent cast scaffolds decreased until weeks 6 and 8 and then increased until its initial value at week 10. The differences in porosity were significant or almost significant ($p < 0.065$) except for the differences between weeks 0 and 2, and weeks 6 and 8 (Figure 4.4). The porosity minimum occurred after six weeks of degradation. The porosity of the phase-separated scaffolds did not vary significantly during the ten weeks of degradation.

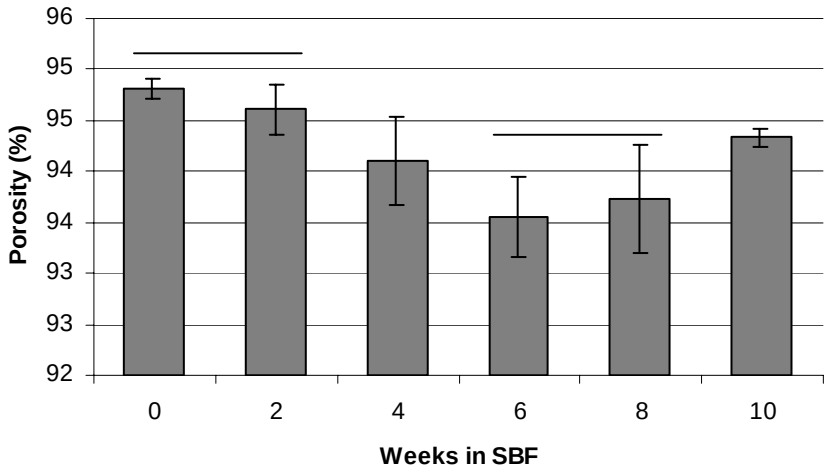

Figure 4.4: Porosity results for the solvent cast scaffolds during the ten-week degradation study. The differences in porosity are not statistically significant between weeks 0 and 2, and weeks 6 and 8.

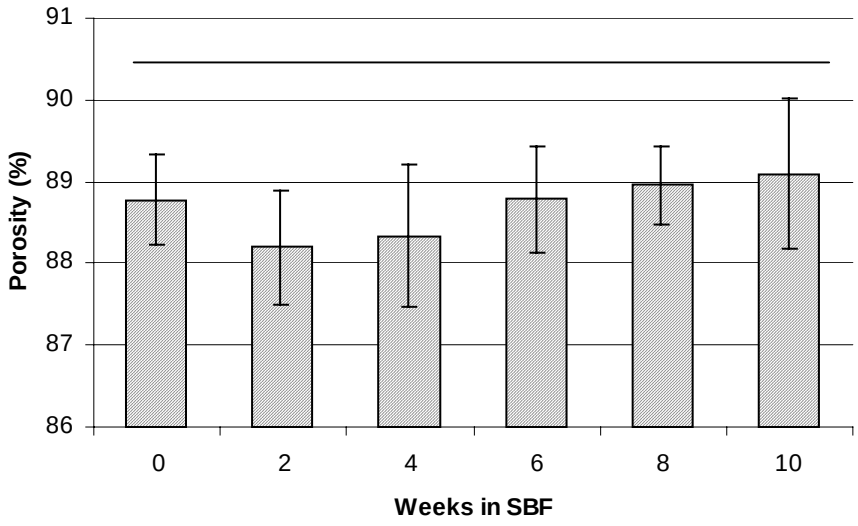

Figure 4.5: Porosity results for the phase-separated scaffolds during the ten-week degradation study. The differences in porosity are not statistically significant.

Mechanical Properties

The stiffness of the solvent cast scaffolds tends to decrease during the ten weeks of degradation in SBF (Figure 4.6), although the difference only becomes statistically significant at week 10. The stiffness of the phase-separated scaffolds, did not vary significantly throughout the assay (Figure 4.7).

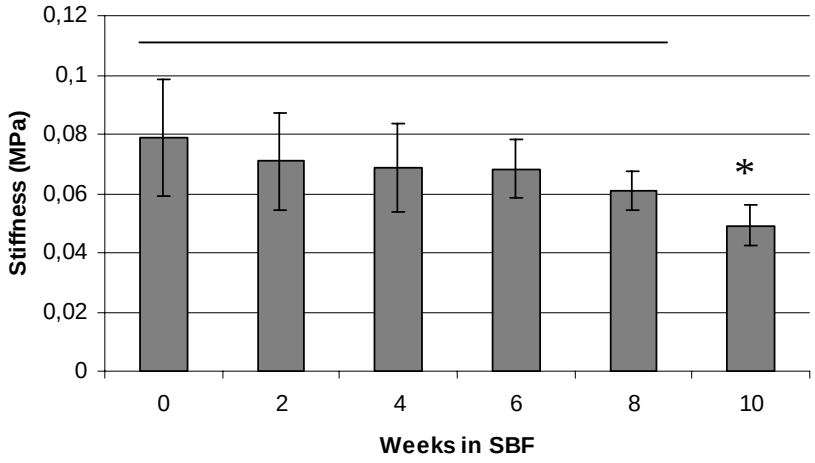

Figure 4.6: Evolution of the stiffness of the solvent cast scaffolds during the ten-week degradation in SBF. Only the difference in stiffness between week 10 and the rest is statistically significant (indicated with an asterix).

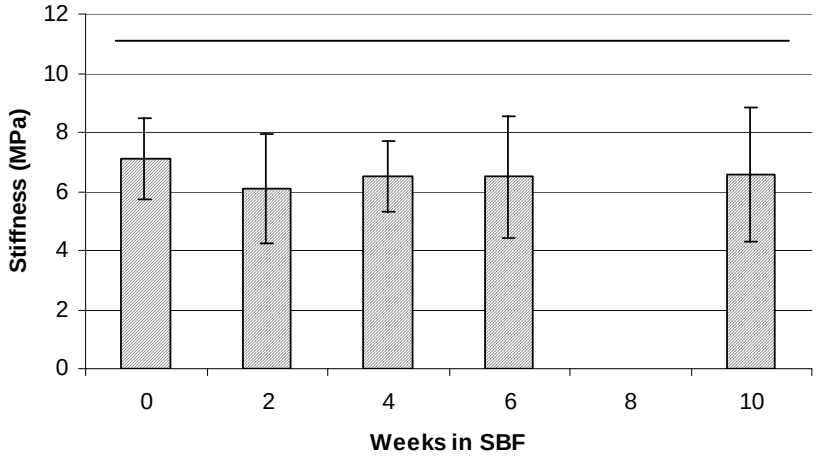

Figure 4.7: Evolution of the stiffness of the phase-separated scaffolds during the ten-week degradation in SBF, there are no significant differences between the values. Due to incorrect handling, the week eight samples crumbled during the tests, their results are not included.

Total Weight Loss

The total weight loss of both types of scaffolds increased steadily during the degradation assay (Figure 4.8). The solvent cast scaffolds lost more weight than the phase-separated ones, and by week ten had crumbled too much to be weighed correctly. Both scaffolds lost approximately 10% of their initial weight during the degradation.

The rate of weight loss followed similar trends for both types of scaffolds; the rate attained a maximum at six weeks of degradation and then decreased (Figure 4.9). The rate of weight loss was higher for the solvent cast scaffolds than for the phase-separated ones.

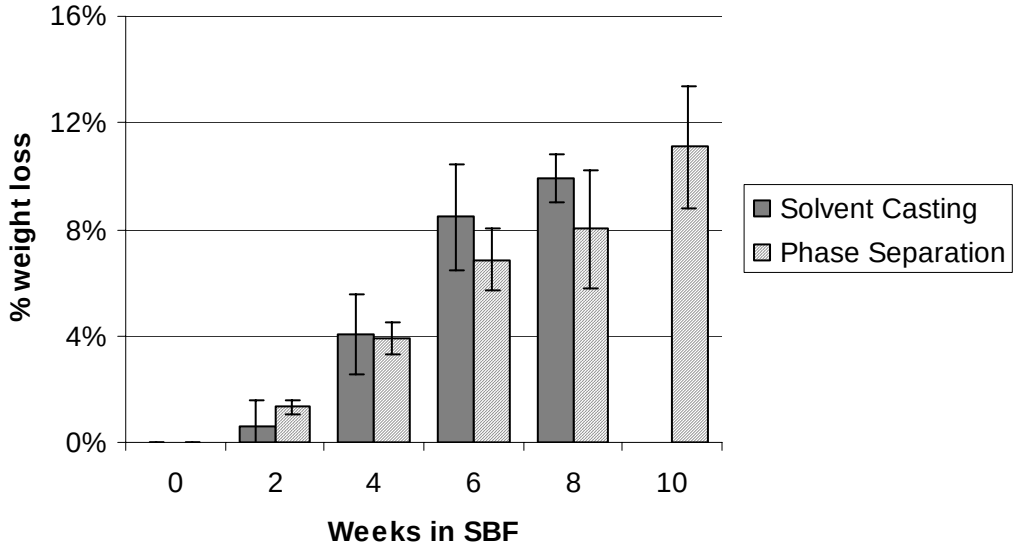

Figure 4.8: Evolution of the percentage weight loss of the solvent cast and phase-separated scaffolds during the ten-week degradation in SBF. The solvent cast scaffolds were too fragile to be weighed correctly at week ten. All differences are statistically significant for both solvent cast and phase-separated scaffolds.

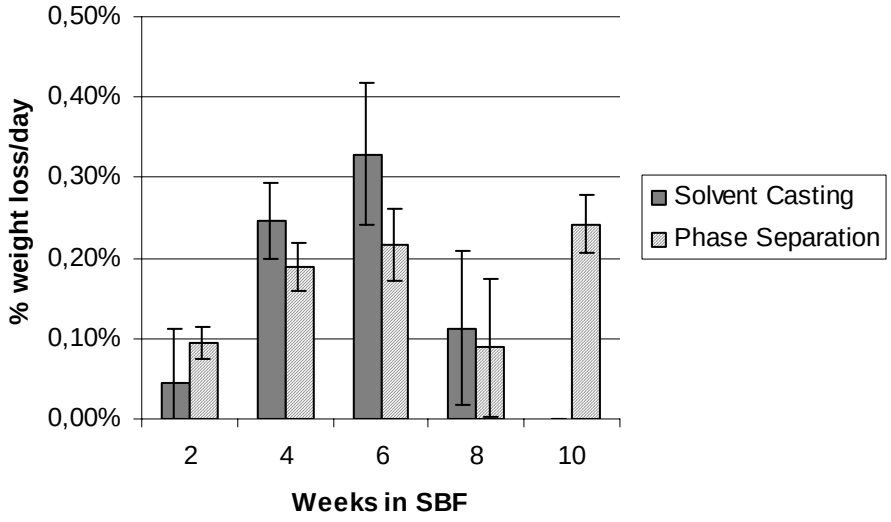

Figure 4.9: Evolution of the rate of weight loss (%weight loss/day) during the ten-week degradation. Each value corresponds to the rate of weight loss during the two previous weeks. They are no readings for the solvent cast scaffolds at week ten because the samples were too fragile to be weighed correctly.

Glass particle content

The percentage of glass particles in the solvent cast scaffolds decreased significantly during the ten weeks of degradation in SBF (Figure 4.10). For the phase-separated scaffolds (Figure 4.11), the glass wt% increased at times, or in other words, the polymer wt% decreased faster than that of the glass. It is interesting to note that the phase-separated scaffolds had a higher initial glass wt% than the solvent cast ones.

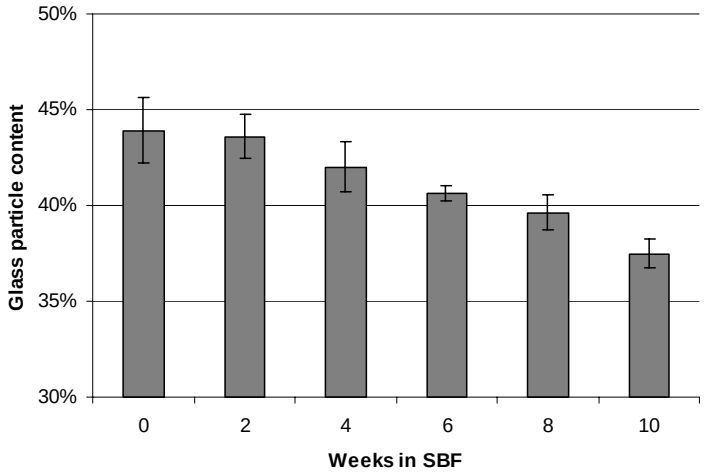

Figure 4.10: Evolution of the glass particle content in the solvent cast scaffolds during the ten-week degradation in SBF. All differences are statistically significant.

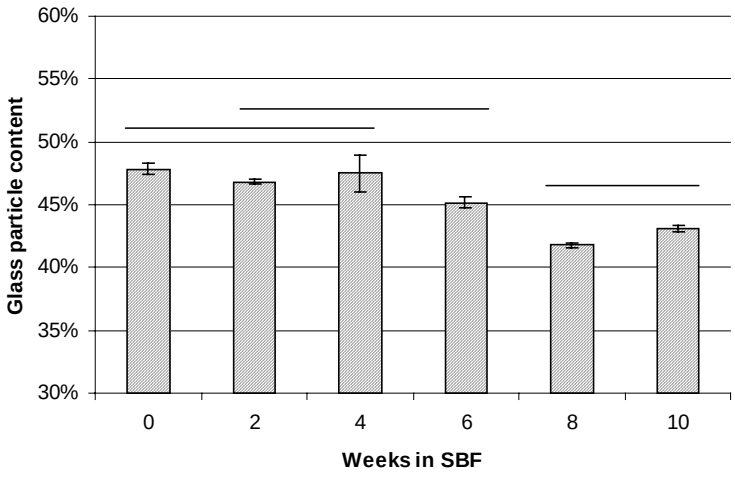

Figure 4.11: Evolution of the glass particle content in the phase-separated scaffolds during the ten-week degradation in SBF.

The total weight loss and the glass particle content have been combined in order to compute the weight loss of glass particles during the ten weeks of degradation (Figure 4.12). Both the solvent cast and phase separated scaffolds have similar glass weight loss profiles (the slope of the curves are almost equal), but the phase-separated scaffolds begin to lose glass two weeks after the solvent cast scaffolds do. Both scaffolds lose almost 20% of their glass weight during the degradation. The total PLA weight loss was less than 5% for both types of scaffolds.

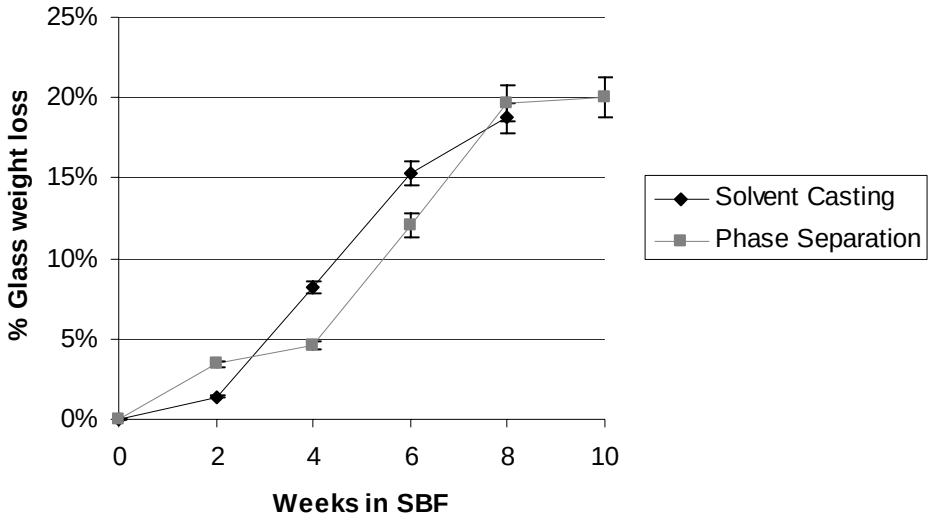

Figure 4.12: Evolution of the glass weight loss during the ten-week degradation in SBF. There are no results for the solvent cast scaffolds at week 10 because the were too fragile to be weighed correctly

Inductively Coupled Plasma readings

The ICP readings are related to the dissolution of the G5 glass in the SBF. Both types of scaffolds gave a maximum ICP reading of approximately 1.3 ppm of titanium ions, though for the solvent cast scaffolds this maximum occurred after two weeks of degradation, whereas it occurred at eight weeks for the phase-separated ones. The ICP readings correspond to the ppm of Ti ions released by the scaffolds during one week of degradation in SBF. All differences are statistically significant.

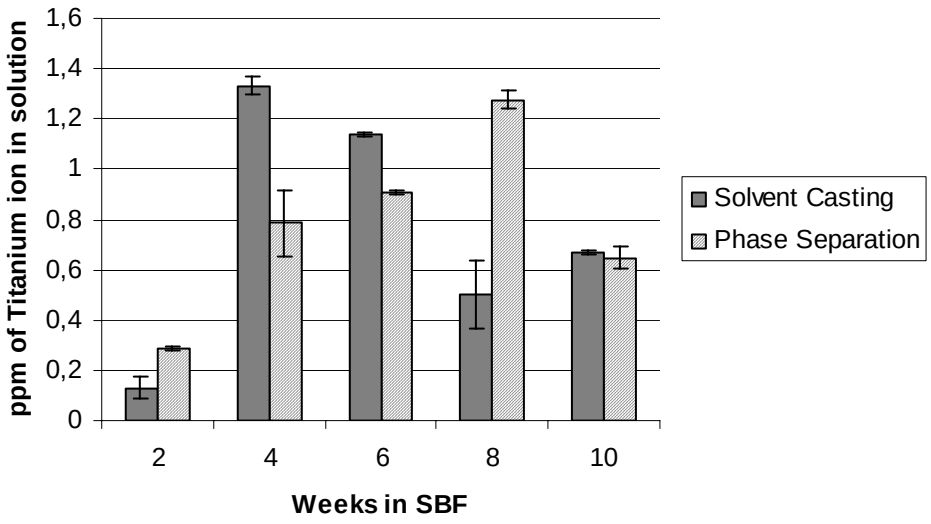

Figure 4.13: Evolution of the ppm of Titanium ion in solution during the ten-week degradation in SBF

Differential Scanning Calorimetry

The DSC scans of the scaffolds were analysed in order to compute their thermal characteristics. The first heating run was used to analyse the T_m and H_f and to calculate the crystallinity of the PLA in the scaffolds. There was no crystallisation peak during the first run, thus the percentage crystallinity was calculated only with the H_f. The second run was used to analyse the T_g and the crystallisability of the PLA by measuring the T_c and H_c.

Typical thermograms of the second heating ramp of the scaffolds during degradation can be seen in Figure 4.14 and Figure 4.15. The crystallisation peak seems to increase in area and decrease in temperature steadily for both types of scaffolds. The melting peak of the thermograms reveals a bimodal melting pattern corresponding to two distinct molecular weights of the PLA.

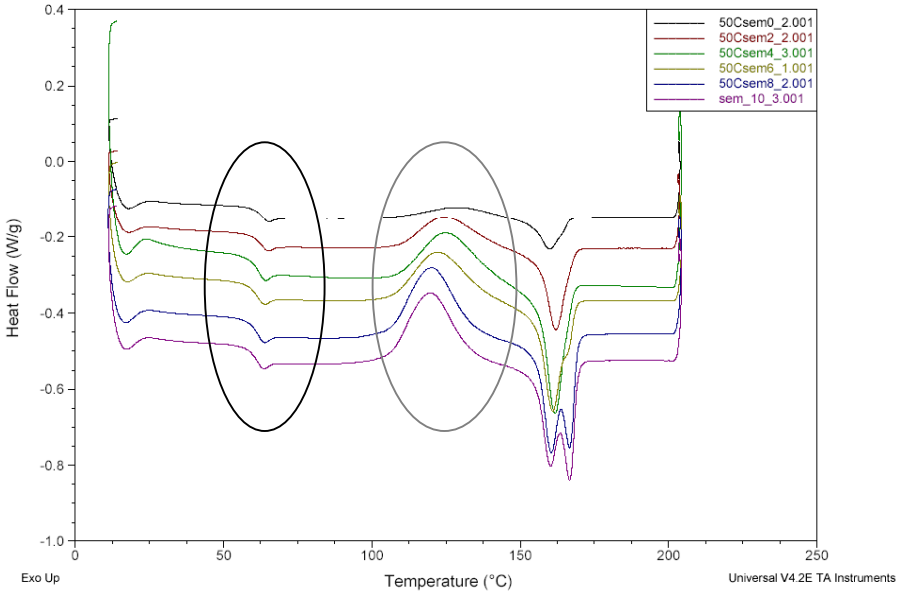

Figure 4.14: Representative thermograms of the second heating ramp of the solvent cast scaffolds during the ten-week degradation in SBF. The black and grey ovals indicate the glass transition and the crystallisation peak respectively.

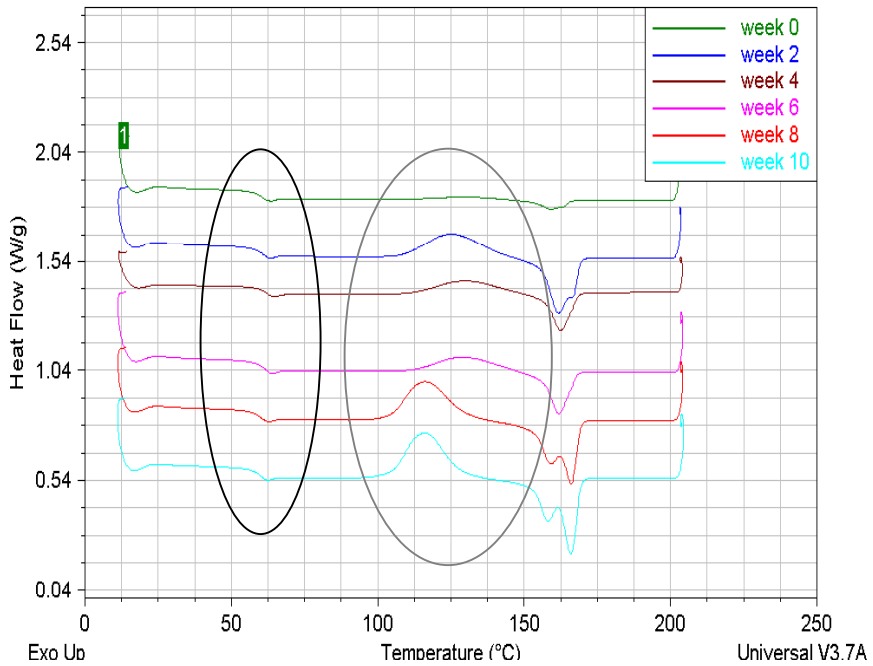

Figure 4.15: Representative thermograms of the second heating ramp of the phase-separated scaffolds during the ten-week degradation in SBF. The black and grey ovals indicate the glass transition and the crystallisation peak respectively.

The thermograms of the first heating ramp can be seen in Figure 4.16 and Figure 4.17. The melting peak is highlighted with a grey oval. For both the solvent cast

and the phase separated scaffolds, the melting peak shifts to slightly higher temperatures and the H_f increases. The quantitative results of the DSC analysis can be seen in the Appendix Chapter 4.

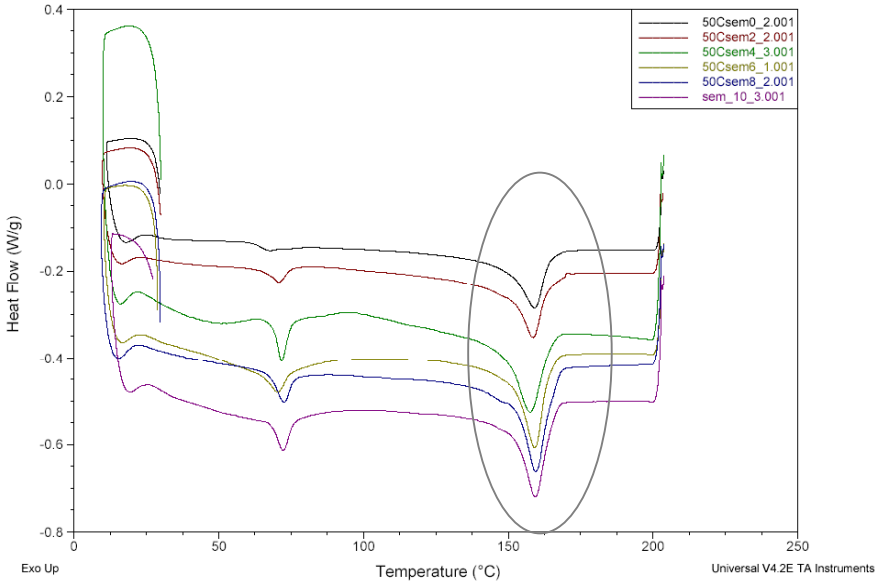

Figure 4.16: Representative thermograms of the first heating ramp of the solvent cast scaffolds during the ten-week degradation in SBF. The black oval indicates the melting peak.

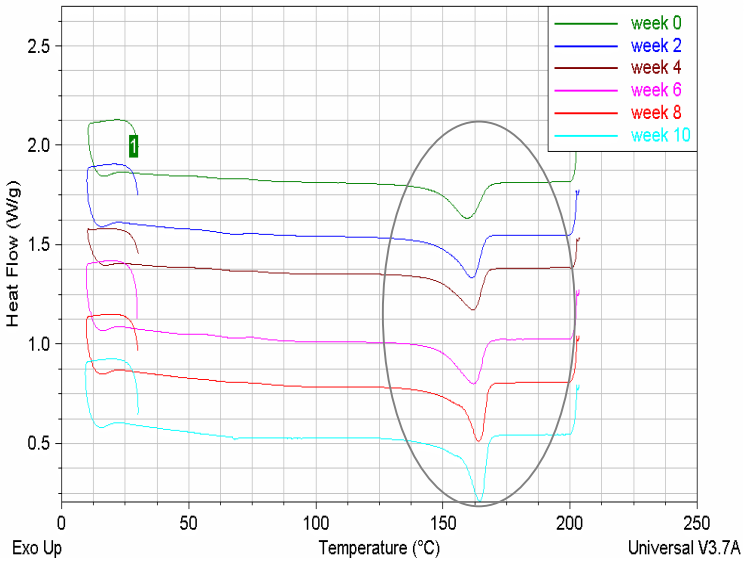

Figure 4.17: Representative thermograms of the first heating ramp of the phase separated scaffolds during the ten-week degradation in SBF. The black oval indicates the melting peak.

Glass TransitionTemperature

The trends in the T_g reading for the solvent cast and phase-separated scaffolds can be seen in Figure 4.18 and Figure 4.19. The T_g of the solvent cast scaffolds decreases very slightly from approximately 63ºC during weeks 0 and 2, to 62ºC from weeks 4 until 10. The T_g of the phase-separated scaffolds seems to increase until week 4 and then decrease, but these differences are not statistically significant.

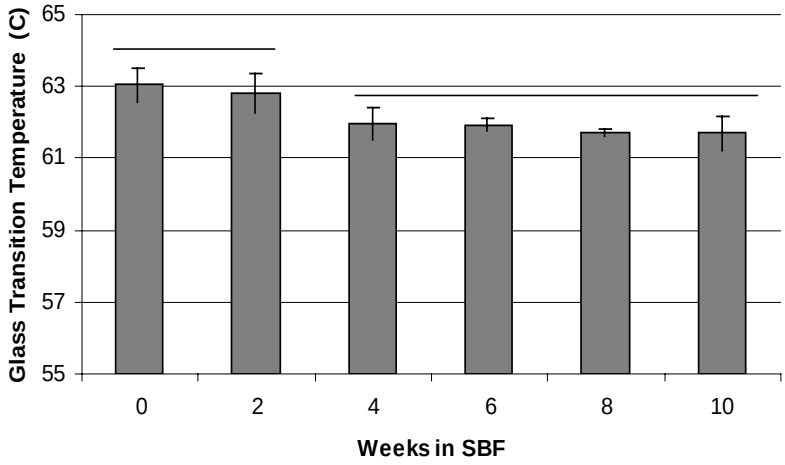

Figure 4.18: Evolution of the Tg of the solvent cast scaffolds during the ten-week degradation in SBF. The differences between weeks 0 and 2, and weeks 4, 6, 8 and 10 are not statistically significant.

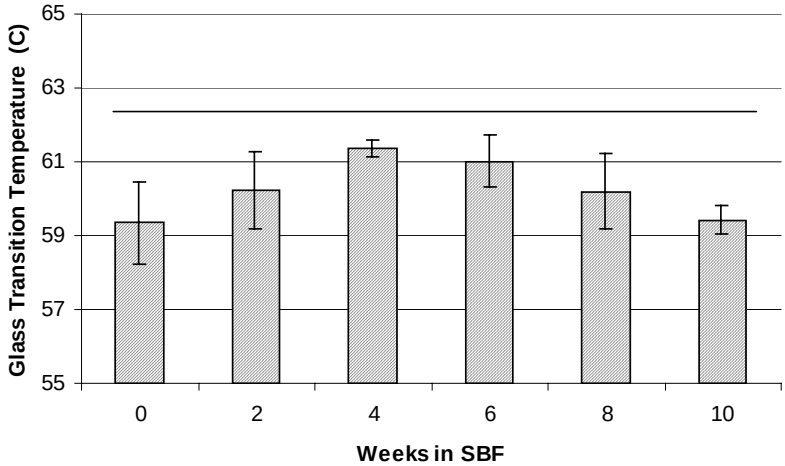

Figure 4.19: Evolution of the Tg of the phase-separated scaffolds during the ten-week degradation in SBF. The differences between the readings are not statistically significant.

Crystallisation Temperature

The evolution of the T_c and H_c of the scaffolds during the second heating ramp can be seen from Figure 4.20 through Figure 4.23. For both types of scaffolds, the H_c increases and the T_c decreases. This means the PLA crystallises more easily as degradation proceeds; it is more "crystallisable".

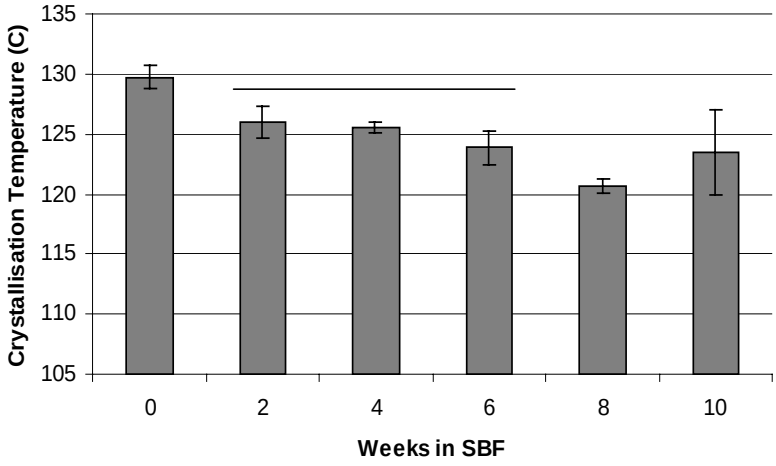

Figure 4.20: Evolution of the crystallisation temperature of the solvent cast scaffolds during the ten-week degradation in SBF. The differences between the readings at week 2, 4 and 6 are not statistically significant.

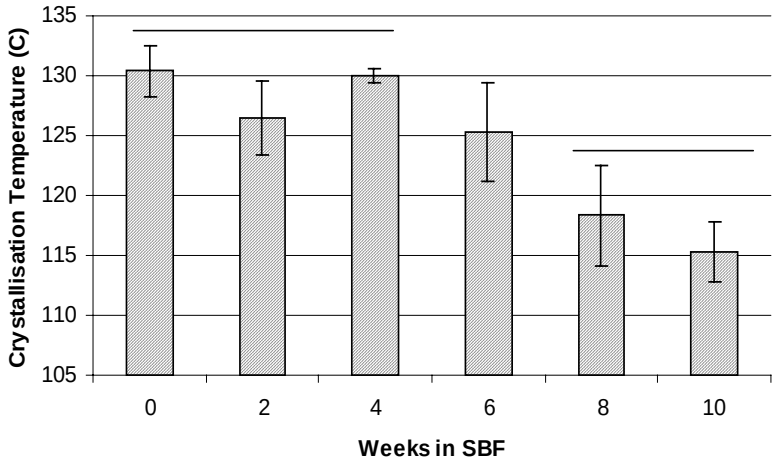

Figure 4.21: Evolution of the crystallisation temperature of the phase-separated scaffolds during the ten-week degradation in SBF. The differences between the readings at weeks 0, 2 and 4, and at weeks 8 and 10 are not statistically significant.

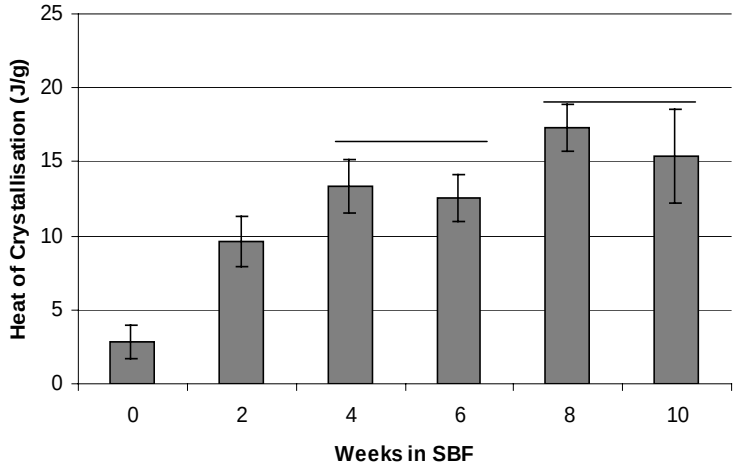

Figure 4.22: Evolution of the crystallisation enthalpy of the solvent cast scaffolds during the ten-week degradation in SBF. The differences between week 4 and 6, and week 8 and 10 are not statistically significant.

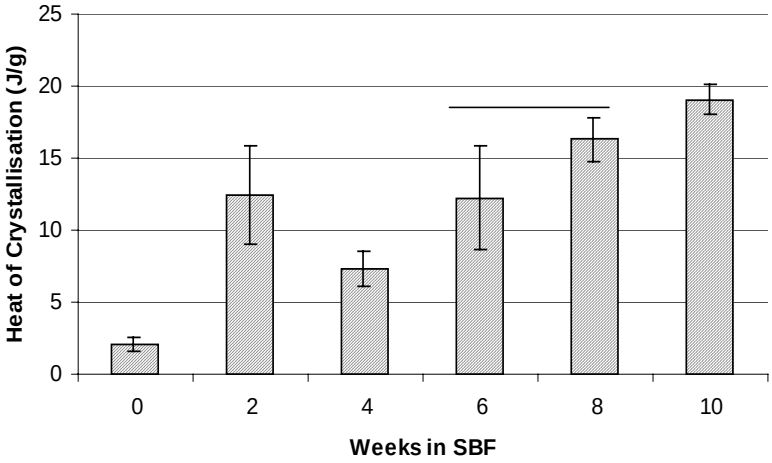

Figure 4.23: Evolution of the crystallisation enthalpy of the phase-separated scaffolds during the ten-week degradation in SBF. The differences between week 6 and 8 are not statistically significant.

Melting and % Crystallinity

The T_m of the PLA in the scaffolds (measured during the first heating ramp) increases with degradation (Figure 4.24 and Figure 4.25). This effect is more pronounced for the phase-separated scaffolds. The H_f also increases with degradation time and is used to calculate the crystallinity, $\%X_c$, of the PLA in the scaffolds (Figure 4.26 and Figure 4.27). The $\%X_c$ of both the solvent cast and phase-separated scaffolds increases during the 10 weeks of degradation; by approximately 9%.

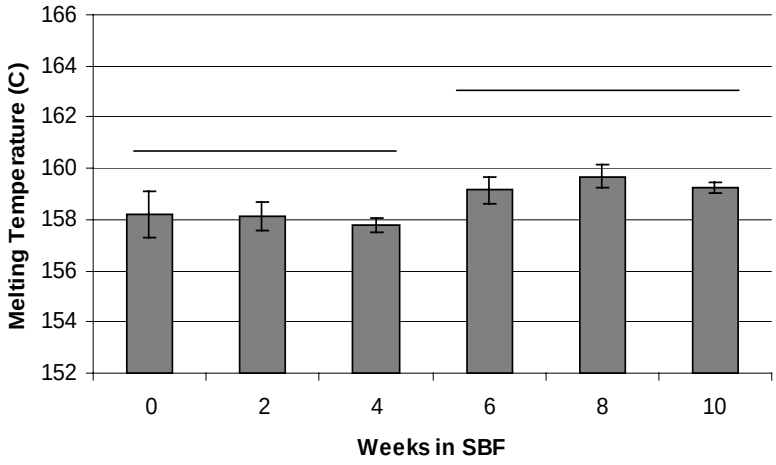

Figure 4.24: Evolution of the melting temperature of the PLA in the solvent cast scaffolds during the ten-week degradation in SBF. The differences between weekd 0, 2 and 4, and weeks 6, 8 and 10 are not statistically significant.

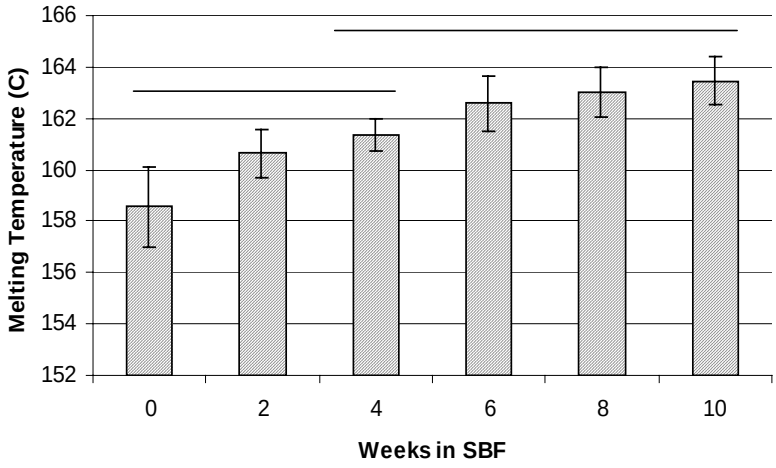

Figure 4.25: Evolution of the melting temperature of the PLA in the phase-separated scaffolds during the ten-week degradation in SBF. The differences between weekd 0, 2 and 4, and weeks 4, 6, 8 and 10 are not statistically significant.

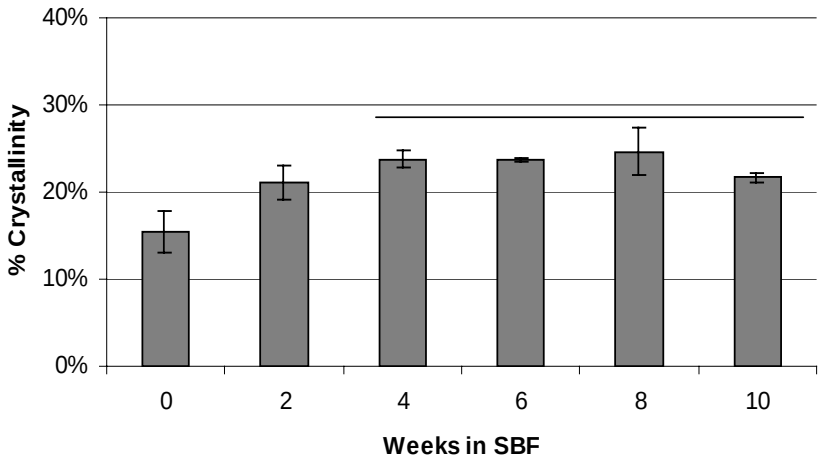

Figure 4.26: Evolution of the crystallinity of the PLA in the solvent cast scaffolds during the ten-week degradation in SBF. The differences between weeks 4 through 10 are not statistically significant.

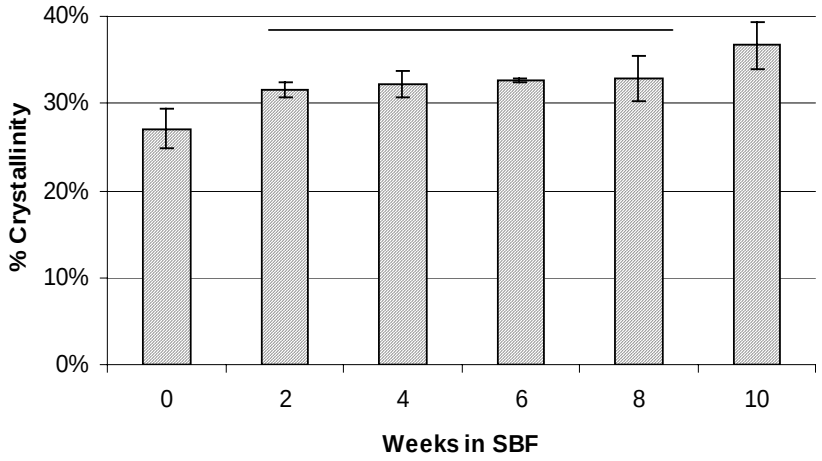

Figure 4.27: Evolution of the crystallinity of the PLA in the phase-separated scaffolds during the ten-week degradation in SBF. The differences between weeks 2 through 8 are not statistically significant.

Discussion

The results of this study indicate that the effect of ten weeks of degradation in SBF on the composite scaffolds depends on how they were manufactured. Although both the solvent cast and phase-separated scaffolds lost weight steadily, SEM imagery, structural analysis and DSC results reveal they are governed by different degradation patterns. Scaffolds made by solvent casting seem to degrade “more” than those made by phase-separation. These results are not surprising, knowing that the processing of the

scaffolds alter many of the factors known to affect PLA degradation as described in Table 4.1 and Table 4.3. First, the degradation of each type of scaffold will be analysed in detail, then they will be compared and discussed.

Degradation has a severe effect on most of the solvent cast scaffold parameters. Qualitative SEM analysis, revealed both the PLA matrix and the glass particles were being degraded. Indeed, the PLA matrix seems to lose some consistency with degradation (Figure 4.2d). The effect of degradation on the glass particles is however, much clearer; Figure 4.2c shows a glass particle in the scaffold exhibiting similar degradation characteristics as those reported by Navarro et al.[14;20] in their *in vitro* degradation tests with the G5 glass. Indeed, their G5 glasses tended to develop a hydrated superficial layer which began to break off in small sheets after ten weeks of degradation in SBF (Figure 4.28). In this case, glass particle degradation refers to the dissolution or loss of weight of glass particles *in vitro*.

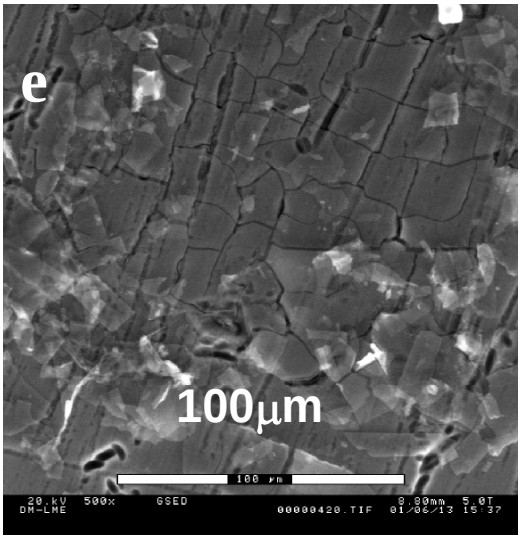

Figure 4.28: Morphology of the surface of the G5 glass after 10 weeks of degradation in SBF. From [20]

The evolution of the structural parameters of the solvent cast scaffolds with degradation time further confirms the qualitative SEM observations. The porosity decreases until week 6 and then increases significantly. This change in trend in porosity may be due to initial water absorption by the PLA matrix. Agrawal et al.[4] report a decrease in the porosity of their scaffolds during the early stages of their dynamic degradation study in PBS. Other authors studying PLA degradation, mention a delay in degradation and the adsorption of water within polymer films at the beginning of

degradation[2]. In the case of the solvent cast scaffolds, the loose PLA-glass interface increases the surface area of PLA exposed to the SBF which could contribute to a higher water absorption.

This decrease in porosity however, does not increase the mechanical properties of the scaffolds. In terms of stiffness, the scaffolds lose 38% of their initial stiffness between week 0 and week 10. This is probably induced by the loss of PLA matrix and especially glass particles during the degradation. In effect the % weight loss and glass particle content show a marked loss of glass particles, which is due to the particles either dissolving or falling-out of the PLA matrix. Thus, the ICP readings include both the glass particles that remain attached to the scaffolds and dissolve, and those that fall out of the scaffolds structure, sink to the bottom of the polyethylene bottle and dissolve. Navarro et al.'s[14] results indicate glass weight loss of less than 1% during 70 days of degradation. Their results, however, refer to the degradation of much larger glass particles (1×1×0.5 cm) which may have slower dissolution kinetics than the glass particles in this study (less than 40μm in diameter). Nevertheless, the large difference between both results indicate the high glass loss rate measured in this study must be partly due to glass particles that have fallen out of the scaffolds. Although glass particles have been shown to weaken the solvent cast scaffold structure (Chapter 2), their falling-out of the structure must leave even more weakening voids. Thus the mechanical weakening of the scaffolds can be attributed to the degradation of the scaffold structure and the loss of the glass particles.

The glass particles in the solvent cast scaffolds tend to fall out of the structure and those that remain are obviously affected by degradation. The PLA matrix seems to suffer less with degradation. Indeed, SEM images and % weight loss rates, indicate that the PLA is far less affected by initial degradation than the glass. Indeed, 20% of the glass weight is lost during the degradation, while the PLA only loses 5% of its initial weight. DSC readings, however, show that the PLA is indeed influenced by the degradation.

The H_c, T_c, and T_g results from the second DSC heating ramp show that the PLA is being attacked hydrolytically and its chains are becoming shorter. This is also evident in the bimodal melting peak shown in Figure 4.14. Furthermore, its $\%X_c$ increases which further demonstrates the higher mobility of the polymer chains. Although T_g

readings are often found to remain unchanged or only decrease slightly in the literature, the differences in ease of crystallisation during the second heating ramp and $\%X_c$ are in full agreement with other studies. Hydrolytic attack on the ester backbone decreases PLA chain length by creating short oligomers or monomers. These oligomers are more mobile and tend to crystallise thus increasing the crystallinity of the PLA. Hydrolysis is also known to attack the amorphous regions of the PLA first, thus increasing the proportion of crystalline regions. Thus the overall crystallinity of the PLA tends to increase during degradation, both due to the selective hydrolytical attack and to the recrystallisation of the oligomers. As a consequence, the molecular weight, M_w, of the PLA also decreases[21;22].

The effect of degradation on the phase-separated scaffolds is far less severe than for the solvent cast scaffolds. Indeed their porosity, qualitative morphology (SEM) and stiffness remain basically unchanged during the ten weeks of degradation in SBF. They do lose weight steadily, however, and again the gross of the weight loss is due to glass particle weight loss. From week four onwards, their weight loss rate is lower than for the solvent cast scaffolds. It is interesting to note that the loss of glass particles does not affect the stiffness of the phase-separated scaffolds significantly.

Again, the DSC readings confirm that the PLA matrix is being degraded although the degradation signs are not very visible. The T_g does not vary significantly, but the ease of crystallisation and the $\%X_c$ do increase. Furthermore, the Tm increases by about 5ºC whereas it only increases 1ºC for the solvent cast scaffolds. Figure 4.15 also reveals a bidmodal melting peak. Thus, it seems the short PLA chains are more mobile in these scaffolds and can increase the crystallinity of the PLA.

The differences between the degradation patterns of the solvent cast and phase-separated scaffolds are most evident in the evolution of their structural parameters. The differences in their T_g, ease of crystallisation and melting characteristics are less marked, but may be responsible for some of the macroscopic differences. The phase-separated scaffolds begin the assay with an average PLA crystallinity of 27%, whereas the solvent cast scaffold matrix is only 12% crystalline. The phase-separated scaffolds are exposed to ethanol during their processing. Ethanol has a plasticising effect on the PLA and is probably responsible for the higher initial crystallinity[27]. Initial

crystallinity reduces the overall degradation rate of the PLA in terms of weight loss and other parameters, given the higher resistance to hydrolytic attack of the crystalline domains[7;23]. Furthermore, the extremely high porosity of the solvent cast scaffolds favours the access of the SBF to the whole scaffold structure. The very weak interface between the glass particles and the PLA creates even more surface area of PLA avaiable to be attacked hydrolytically.

Thus, the solvent cast PLA matrix should be more prone to hydolysis, and should begin degrading before the phase-separated one. Indeed, the decrease in porosity of the solvent cast scaffolds, probably due to the absorption of water, confirms this idea. As does the slight decrease in T_g after week two. Furthermore, the increase in $\%X_c$ of the solvent cast scaffolds is slightly higher than for the phase-separated ones, indicating either a higher loss of amorphous regions, or the presence of more short crystallisable oligomers. After ten weeks of degradation, however, both types of scaffolds had lost the same percentage of PLA weight (<5%). And many authors find little or no weight loss in their polymeric scaffolds during the first 15-20 weeks of degradation[2;10], whereas others report weight losses of up to 70%[3].

Thomson et al.[24] report a decrease in the mechanical properties of their scaffolds with decreasing polymer molecular weight. The increase in crystallinity and the bimodal melting peaks of both types of scaffolds (Figure 4.14 and Figure 4.15), indicates they are both undergoing chain scission and thus decreasing their molecular weight. The lower melting point of the solvent cast scaffolds as opposed to the phase-separated ones, (Figure 4.24) could indicate a lower M_w for the solvent cast scaffolds which could be responsible for the loss of mechanical properties. This hypothesis cannot be confirmed though, due to the absence of molecular weight analysis, and its effect could not explain the big difference in trend between the two. Indeed, most molecular weight analysis techniques require separating the PLA from the glass particles by dissolving the PLA in a solvent and filtering the solution. This technique is, however, not straightforward and was not possible for this study.[11;25;26]

Given that for both scaffolds the PLA matrices evolve in basically the same way, the loss of stiffness of the solvent cast scaffolds must be due to their structure and the effect of the loss of glass particles. ICP readings and %glass weight loss (Figure 4.13 and Figure 4.12) show the initial glass loss is greater for the solvent cast scaffolds, but

the total losses level out after ten weeks of degradation. The faster glass loss in the solvent cast scaffolds must be due to the fact that the glass particles are more exposed to the SBF than in the phase-separated scaffolds. What may be true, is that the effect of the glass particle loss is more severe on the solvent cast scaffold structure. Perhaps due to the very thin pore walls and the voids the glass particles must leave behind after falling out. The exact amount of glass particles that fell out of the scaffolds could not be measured. Various attempts to filter the solution and calcinate the filter to be able to calculate the amount of glass particles that fell out of the scaffolds proved unfruitful. The glass particles tended to clog the filter which in turn created problems with the vacuum pump used to force the filtering. Besides, a visible amount of glass remained within the tubes and vessels of the filtering system.

In sum, the onset of degradation occurs earlier for the solvent cast scaffolds and the loss of glass particles proves more fatal for them. Perhaps their highly porous structure makes them weaker and more sensitive to the effects of degradation.

Some limitations to this study have been mentioned above; the lack of molecular weight measurements and the uncertainty about the glass particle behaviour. In addition, the static conditions of the assay could create extreme concentrations or pH's which could exaggerate or alter the normal degradation pattern of the scaffolds. Some areas which could be further explored would be the effect of the ultraviolet radiation on the scaffolds properties, the effect of the SBF pH, and the occurrence of calcium phosphate precipitates at different w/v ratios.

The results, however, do offer a broad characterisation of the degradative pattern of the PLA in the scaffolds and have clearly pointed out the higher susceptibility of the solvent cast scaffolds to degradation. The results also confirm the qualitative observation during sample handling, that the solvent cast scaffolds, were crumbling and losing consistency towards the end of the degradation experiment, whereas the phase-separated scaffolds seem basically intact. Increasing the degradation period, could offer further information on scaffold behaviour, but given the differences between *in vivo*, cellular *in vitro*, and acellular *in vitro* conditions, the next step in degradation studies, should perhaps be performed with cell cultures, evaluating the materials' effect on cellular behaviour. Navarro et al.[28] confirmed these materials were not cytotoxic.

Thus the next step of this study is to perform cell cultures and better understand the scaffolds' interaction with cells.

Conclusions

- A characterisation of the degradation of the solvent cast and phase-separated scaffolds was performed in this study. The parameters involved, gave information on the evolution of the morphology, mechanical properties, and porosity, as well as the degradation of the PLA and the glass particles.
- The results show a very clear effect of the manufacturing procedure on the degradation of the scaffolds: solvent cast scaffolds were degraded far more severely than the phase-separated ones.
- The effects of degradation were evident for solvent cast scaffolds in their SEM images, porosity and mechanical properties.
- The DSC readings revealed the PLA followed its typical degradation pattern: the crystallinity and crystallisability increased. Despite the absence of direct readings, the molecular weight seems to decrease.
- Weight loss and calcination results give evidence of a large loss of glass particles during degradation. The glass particles seem to fall out of the scaffold structure. The effect of this glass particle release should be evaluated *in vivo*.
- The characterisation of the degradation properties of these composite materials will be a valuable tool to couple with cell culture assays in order to understand their biological behaviour (Chapter 6).

Bibliography

(1) Navarro M, Aparicio C, Charles-Harris M, Ginebra MP, Engel E, Planell JA. Development of a biodegradable composite scaffold for bone tissue engineering: physico-chemical, topographical, mechanical, degradation and biological properties. Advances in Polymer Science 2006; 200:209-231.

(2) Holy CE, Dang SM, Davies JE, Shoichet MS. In vitro degradation of a novel poly(lactide-co-glycolide) 75/25 foam. Biomaterials 1999; 20(13):1177-1185.

(3) Marra KG, Szem JW, Kumta PN, DiMilla PA, Weiss LE. In vitro analysis of biodegradable polymer blend/hydroxyapatite composites for bone tissue engineering. J Biomed Mater Res 1999; 47:324-335.

(4) Agrawal CM, McKinney JS, Lanctot D, Athanasiou KA. Effects of fluid flow on the in vitro degradation kinetics of biodegradable scaffolds for tissue engineering. Biomaterials 2000; 21(23):2443-2452.

(5) Roether JA, Boccaccini AR, Hench LL, Maquet V, Gautier S, Jérôme R. Development and in vitro characterisation of novel bioresorbable and bioactive composite materials based on polylactide foams and Bioglass for tissue engineering applications. Biomaterials 2002; 23:3871-3878.

(6) Murphy WL, Kohn DH, Mooney DJ. Growth of continuous bonelike mineral within porous poly(lactide-co-glycolide) scaffolds in vitro. J Biomed Mater Res 2000; 50(1):50-58.

(7) Li S. Hydrolytic degradation characteristics of aliphatic polyesters derived from lactic and glycolic acids. J Biomed Mater Res 1999; 48(3):342-353.

(8) von Recum HA, Cleek RL, Eskin SG, Mikos AG. Degradation of polydispersed poly(L-lactic acid) to modulate lactic acid release. Biomaterials 1995; 16(6):441-447.

(9) Grizzi I, Garreau H, Li S, Vert M. Hydrolytic degradation of devices based on poly(DL-lactic acid) size-dependence. Biomaterials 1995; 16(4):305-311.

(10) Lu L, Peter SJ, Lyman MD, Lai HL, Leite SM, Tamada JA, Uyama S, Vacanti JP, Langer R, Mikos AG. In vitro and in vivo degradation of porous poly(DL-lactic-co-glycolic acid) foams. Biomaterials 2000; 21(18):1837-1845.

(11) Vert M, Schwach G, Engel R, Coudane J. Something new in the field of PLA/GA bioresorbably polymers? Journal of Controlled Release 1998; 53:85-92.

(12) Gopferich A. Mechanisms of polymer degradation and erosion. Biomaterials 1996; 17(2):103-114.

(13) Clement J, Avila G, Navarro M, Martinez S, Ginebra MP, Planell JA. Chemical Durability and Mechanical Properties of Calcium Phosphate Glasses with the Addition of Fe_2O_3, TiO_2 and ZnO. Key Engineering Materials 2001; 192-195:621-624.

(14) Navarro M, Ginebra MP, Clement J, Martinez S, Avila G, Planell JA. Physicochemical degradation of titania-stabilized soluble phosphate glasses for medical applications. Journal of the American Ceramic Society 2003; 86(8):1345-1352.

(15) Kokubo T, Kushitani H, Sakka S, Kitsugi T, Yamamuro T. Solutions able to reproduce in vivo surface-structure changes in bioactive glass-ceramin A-W. J Biomed Mater Res 1990; 24:721-734.

(16) Kokubo T, Takadama H. How useful is SBF in predicting in vivo bone bioactivity? Biomaterials 2006; 27(15):2907-2915.

(17) Takadama H, Hashimoto M, Mizuno M, Ishikawa K, Kokubo T. Newly improved simulated body fluid. Bioceramics 16 2004; 254-2:115-118.

(18) UNE 53-090 Determinación del contenido en cenizas de materiales plásticos. Norma Española 1976.

(19) Fischer EW, Sterzel HJ, Wegner G. Investigation of the structure of solution grown crystals of lactide copolymers by means of chemical reactions. Kolloid-Zeitschrift and Zeitschrift fur Polymere 1973; 251:978-990.

(20) Navarro M. Desarrollo y caracterización de materiales biodegradables para regeneración ósea. UPC, 2005.

(21) Landes CA, Ballon A, Roth C. In-patient versus in vitro degradation of P(L/DL)LA and PLGA. J Biomed Mater Res B Appl Biomater 2006; 76(2):403-411.

(22) Leenslag JW, Pennings AJ, Bos RR, Rozema FR, Boering G. Resorbable materials of poly(L-lactide). VII. In vivo and in vitro degradation. Biomaterials 1987; 8(4):311-314.

(23) Jamshidi K, Hyon S-H, Ikada Y. Thermal characterization of polylactides. Polymer 1988; 29:2229-2234.

(24) Thomson RC, Yaszemski MJ, Powers JM, Mikos AG. Fabrication of biodegradable polymer scaffolds to engineer trabecular bone. J Biomater Sci Edn 1995; 7(1):23-38.

(25) Schmitt EA, Flanagan DR, Linhardt RJ. Importance of distinct water environments in the hydrolysis of poly(DL.lactide-co-glycolide). Macromolecules 1994; 27:743-748.

(26) Bergsma JE, Rozema FR, Bos RRM, Rozendaal AWM, de Jong WH, Teppema JS, Joziasse CAP. Biocompatibility and degradation mechanisms of predegraded and non-predegraded poly(lactide) implants: an animal study. Journal of Materials Science: Materials in Medicine 1995; 6:715-724.

(27) Blasi P, D'Souza SS, Selmin F, DeLuca PP. Plasticizing effect of water on poly(lactide-co-glycolide). J Control Release 2005; 108(1):1-9.

(28) Navarro M, Ginebra MP, Planell JA, Zeppetelli S, Ambrosio L. Development and cell response of a new biodegradable composite scaffold for guided bone regeneration. J Mater Sci Mater Med 2004; 15(4):419-422.